Portugaliae Electrochimica Acta 2013, 31(3), 141-155

DOI: 10.4152/pea.201303141

PORTUGALIAE ELECTROCHIMICA ACTA
ISSN 1647-1571

Inhibition of Corrosion of Carbon Steel in Sea Water by Sodium Gluconate - Zn^{2+} System

S. Rajendran,[a] K. Anuradha,[b] K. Kavipriya,[a,*] A. Krishnaveni,[c] J. Jeyasundari[d] and V. Sribharathy[a]

[a] *Corrosion Research Center, PG and Research Department of Chemistry, GTN Arts College, Dindigul 624 005, Tamilnadu, India*
[b]*Department of Chemistry, KLN College of Information Technology, Pottapalayam 630 611, India*
[c]*Department of Chemistry, Yadava Collge, Madurai, India*
[d] *Department of Chemistry, SVN College, Madurai, India*

Received 19 May 2012; accepted 27 June 2013

Abstract

The inhibition efficiency of sodium gluconate (SG)–Zn^{2+} system in controlling corrosion of carbon steel in sea water has been evaluated by weight-loss method. The formulation consisting of 250 ppm of SG and 75 ppm of Zn^{2+} has 98% IE. Influence of duration of immersion on the IE of SG-Zn^{2+} has been evaluated. The mechanistic aspects of corrosion inhibition have been investigated by polarization study and AC impedance spectra. The protective film has been analysed by FTIR and luminescence spectra. The surface morphology and the roughness of the metal surface have been analysed by atomic force microscopy. The protective film consists of Fe^{2+} - SG complex and $Zn(OH)_2$. It is found to be UV – fluorescent.

Keywords: Carbon steel, sodium gluconate, synergistic effect, Atomic Force Microscopy (AFM), Fourier Transform Infrared Spectroscopy (FTIR), corrosion.

Introduction

Several carboxylic acids have been used as corrosion inhibitors to prevent corrosion of metals [1-35]. Their inhibitive action is due to coordination of the oxygen atom of the carboxylate anion to the metal ions to form metal–inhibitor complexes. They have been used to prevent the corrosion of metals such as mild steel [1, 10, 11, 14, 32, 33], aluminium [7, 9] and copper [19, 23].

* Corresponding author. E-mail address: sennikavi@yahoo.co.in

The environment includes various media like acidic [6, 12, 23, 33], alkaline [6] and neutral [8, 9, 10, 12]. Thermodynamic studies [19], quantum chemical studies [35], and electrochemical studies [4] have been employed to explain the inhibitive actions of carboxylic acids. Phosphono carboxylic acids [29, 31, 32], tartrates [8, 10], amino acids [19] and citrates [1] have been used as corrosion inhibitors.

The present work is undertaken (i) to evaluate the inhibition efficiencies of sodium gluconate (SG)–Zn^{2+} system in controlling corrosion of carbon steel in sea water by weight-loss method, (ii) to investigate the mechanistic aspects of corrosion inhibition by electrochemical studies like polarization study and AC impedance spectra, (iii) to analyse the protective film by FTIR and luminescence spectra, (iv) to analyse the surface morphology by AFM, and (v) to propose a suitable mechanism of corrosion inhibition based on the results from the above study.

Experimental

Preparation of specimens

Carbon steel specimens [0.0267 % S, 0.06 % P, 0.4 % Mn, 0.1 % C and the rest iron] of dimensions 1.0 cm x 4.0 cm x 0.2 cm were polished to a mirror finish and degreased with trichloroethylene.

Weight-loss method

Carbon steel specimens in triplicate were immersed in 100 mL of solutions containing various concentrations of the inhibitor in the presence and absence of Zn^{2+} for one day. The weight of the specimens before and after immersion was determined using a Shimadzu balance, model AY62. The corrosion products were cleansed with Clarke's solution [36]. The inhibition efficiency (IE) was then calculated using the equation.

$$IE = 100\ [1- (W_2 / W_1)]\ \%$$

where W_1 = corrosion rate in the absence of the inhibitor, and W_2 = corrosion rate in the presence of the inhibitor.

Biocidal study

Inhibitor – Zn^{2+} formulations that offered the best corrosion inhibition efficiency were selected for biocidal study. The biocidal efficiency of N- cetyl –N, N, N – trimethylammonium bromide (CTAB) in the presence and absence of these formulations and also the effect of CTAB on the corrosion inhibition efficiency of these systems were determined [37-39].

Various concentrations of CTAB 50 ppm, 100 ppm, 150 ppm, 200 ppm, and 250 ppm were added to the formulation consisting of the inhibitor system. The numbers of colony-forming units (CFU/mL) present in the above formulation were determined by step dilution technique. Synergistic formulations were taken into Petri dishes and mixed with 15 mL of sterile nutrient agar. While mixing,

the plate was tilted back and forth, so that the medium and sample travels around the plate several times. Then, the Petri dishes were kept in an incubator at 30 ^{o}C in an inverted position for 5 days. Distinct colonies of bacteria were developed. Such colonies may be easily isolated. Each organism grew and reproduced itself. To determine the number of colonies, the plate count technique was applied. One organism gives rise to one colony. Hence, a colony count performed on the plate reveals the viable microbial population. Within the range of 30-300, the count can be accurate. Colonies are usually counted from dark field illumination, so that they are easily visible and a large magnifying lens is often used. Number of colonies counted on plate x dilution of sample = number of bacteria per mL.

Surface examination study

The carbon steel specimens were immersed in various test solutions for a period of one day. After one day, the specimens were taken out and dried. The nature of the film formed on the surface of the metal specimens was analysed for surface analysis technique by FTIR spectra and fluorescence spectra.

FTIR spectra

The film formed on the metal surface was carefully removed and mixed thoroughly with KBr. The FTIR spectra were recorded in a Perkin Elmer 1600 spectrophotometer.

Fluorescence spectra

These spectra were recorded in a Hitachi F-4500 fluorescence spectrophotometer.

Atomic Force Microscopy

Atomic Force Microscopy (AFM) is an exciting new technique that allows surface to be imaged at higher resolutions and accuracies than ever before [40-42]. The microscope used for the present study was PicoSPM I Molecular Imaging, USA. Polished specimens prior to the initiation of all corrosion experiments were examined through an optical microscope to find out any surface defects such as pits or noticeable irregularities like cracks, etc. Only those specimens which had a smooth pit-free surface were subjected for AFM examination. The protective films formed on the carbon steel specimens after immersion in the inhibitor systems for different time durations were examined for a scanned area of 30 x 30 μm^2 and 15 x 15 μm^2. The two-dimensional and three-dimensional topographies of surface films gave various roughness parameters of the film.

Polarization study

Polarization studies were carried out in an H & CH electrochemical workstation impedance analyser, model CHI 660A.

A three-electrode cell assembly was used. The working electrode was carbon steel. A saturated calomel electrode (SCE) was used as the reference electrode and a rectangular platinum foil was used as the counter electrode.

AC impedance measurements

The instrument used for polarization study was used for AC impedance measurements too. The cell set up was the same as that used for polarization measurements. The real part (Z') and the imaginary part (Z") of the cell impedance were measured in Ohms at various frequencies. The values of charge transfer resistance, R_t, and the double layer capacitance, C_{dl}, were calculated.

$$R_t = (R_s + R_t) - R_s$$

where R_s = solution resistance, and

$C_{dl} = 1 / 2\ \Pi\ R_t\ f_{max}$

being f_{max} = maximum frequency.

Results and discussion

The inhibition efficiency of sodium gluconate (SG)–Zn^{2+} system in controlling corrosion of carbon steel in sea water (Table 1) has been evaluated by weight-loss method and electrochemical studies such as potentiodynamic polarization study and AC impedance spectra.

Table 1. Characteristics of sea water collected from Tiruchendur, in Thoothukudi District, Tamilnadu, India.

Parameter	Value
Total dissolved salts (mg/L)	41.600
Electrical conductivity (micro mhos/cm)	64.000
pH	7.4
Total hardness ($CaCO_3$ equivalent)	4000
Calcium as Ca (mg/L)	600
Magnesium as Mg (mg/L)	600
Sodium as Na (mg/L)	8900
Chloride as Cl (mg/L)	20.750
Fluoride as F (mg/L)	1.5
Free ammonia as NH_3 (mg/L)	0.09
Sulphate as SO_4 (mg/L)	2332

Weight-loss method

Inhibition efficiencies (IE %) of SG–Zn^{2+} systems in controlling corrosion of carbon steel in sea water (immersion period = 5 days) are given in Table 2. It is observed that SG alone has good inhibition efficiency. As the concentration of SG increases, the IE also increases.

In the presence of various concentrations of Zn^{2+} (25, 50 and 75 ppm), the IE of SG increases. A synergistic effect exists between SG and Zn^{2+}. For example, 250 ppm of SG have only 61% IE; 75 ppm of Zn^{2+} have 39% IE. However, their combination has 98% IE. This suggests a synergistic effect existing between SG and Zn^{2+}.

Table 2. Inhibition efficiency (IE %) offered by sodium gluconate (SG)–Zn^{2+} system to carbon steel in sea water, obtained by weight-loss method. Duration of immersion = 5 days.

SG ppm	Zn^{2+}, ppm			
	0	**25**	**50**	**75**
0	-	13	20	39
50	20	25	20	68
100	30	36	28	75
150	42	44	33	87
200	53	56	56	90
250	61	65	70	98

Influence of duration of immersion on the inhibition efficiency of the SG-Zn^{2+} system

The formulation consisting of 250 ppm SG and 50 ppm of Zn^{2+} has 98% IE (immersion period = 5 days). The influence of the immersion period on the IE of this system is shown in Fig. 1. It is observed that the IE almost remains constant up to 5 days. Afterwards, the IE decreases. On the seventh day, the IE decreases from 98% to 92%. This is due to the fact that as the immersion period increases, the protective film formed on the metal surface, namely, Fe^{2+}–SG complex, is broken by the aggressive chloride ions present in sea water and hence the IE decreases. Further, a competition arises between the formation of Fe^{2+}–SG complex and $FeCl_2$/$FeCl_3$. As the immersion period increases, the formation of $FeCl_2$/$FeCl_3$ is favoured to Fe^{2+}–SG complex at the anodic sites of the metal and hence the IE decreases [43].

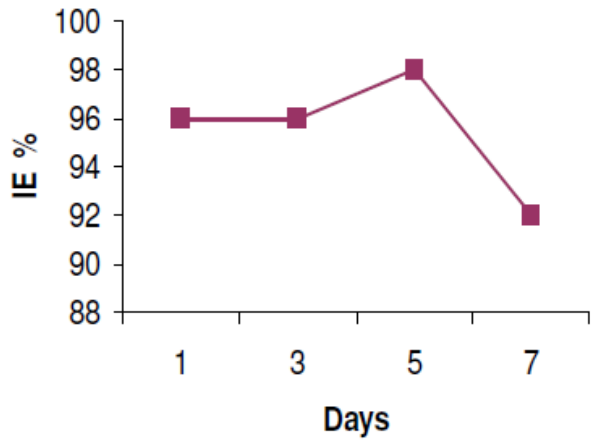

Figure 1. Influence of duration of immersion on the IE of the SG (250 ppm) + Zn^{2+} (75 ppm) system.

Synergism parameters

Synergism parameter (S_I) has been calculated to know the synergistic effect existing between two inhibitors [44-47]. Synergism parameter is calculated using the relation

$$S_I = \frac{1 - \theta_{1+2}}{1 - \theta'_{1+2}}$$

where $\theta_{1+2} = (\theta_1 + \theta_2) - (\theta_1 * \theta_2)$, θ is the surface coverage of inhibitor (=IE%/100), and θ_1 and θ_2 are the surface coverage of inhibitor 1 and 2, respectively:

$$\theta'_{1+2} = \frac{\text{Combined IE\%}}{100}$$

= combined surface coverage in presence of inhibitors 1 and 2.

When a synergistic effect exists between two inhibitors, the synergism parameter will be greater than 1. It is observed from Table 3, that the S_I values are greater than 1. This confirms the synergistic effect existing between SG and Zn^{2+}. As a model, the Zn^{2+} (75 ppm)-SG (50, 100, 150, 200 and 250 ppm) system has been selected to evaluate the synergism parameters.

Table 3. Synergism parameters (S_I) of SG (50, 100, 150, 200, 250 ppm) – Zn^{2+} (75 ppm) system.

SG ppm	IE% I_1	Zn^{2+} ppm	IE% I_2	Combined IE% I'_{1+2}	Synergism parameter S_I
50	20	75	39	68	1.53
100	30	75	39	75	1.71
150	42	75	39	87	2.72
200	53	75	39	90	2.87
250	61	75	39	98	13.95

Influence of N-cetyl-N, N, N-trimethylammoniam bromide (CTAB) on the corrosion inhibition efficiency of the SG–Zn^{2+} system

CTAB is a cationic surfactant. It is a biocide [37-39].

The influence of CTAB on the corrosion inhibition efficiency (IE %) of the SG (250 ppm) -Zn^{2+} (75 ppm) system and also the influence of SG-Zn^{2+} system on the biocidal efficiency (BE) of the CTAB system have been evaluated by weight-loss method and also by calculating the number of colony-forming units. It is observed from Table 4 that the formulation consisting of 250 ppm of SG, 75 ppm of Zn^{2+} and 250 ppm of CTAB has 91% corrosion inhibition efficiency and 100% biocidal efficiency. This formulation may find application in cooling water systems, if further research is carried out at high temperature under flow condition.

Table 4. Influence of CTAB on the corrosion inhibition efficiency of the SG (250 ppm) + Zn^{2+} (75 ppm) system.

SG ppm	Zn^{2+} ppm	CTAB ppm	CR mdd	IE %	Colony forming units/mL	Biocide efficiency (BE)%
0	0	0	18.18	-	13.3×10^3	-
250	75	0	0.36	98	1.9×10^3	86
250	75	50	2.36	87	Nil	78
250	75	100	5.27	71	Nil	100
250	75	150	6.18	66	Nil	100
250	75	200	2.91	84	Nil	100
250	75	250	1.64	91	Nil	100

Potentiodynamic polarization study

Polarization study has been used to confirm the formation of a protective film on the metal surface [48-52]. If a protective film is formed on the metal surface, the linear polarization resistance value (LPR) increases and the corrosion current value (I_{corr}) decreases.

The polarization curves of carbon steel immersed in sea water in presence of the inhibitor system are shown in Fig. 2. The corrosion parameters, namely corrosion potential (E_{corr}), Tafel slopes (b_c = cathodic; b_a = anodic), LPR values and I_{corr} values are given in Table 5.

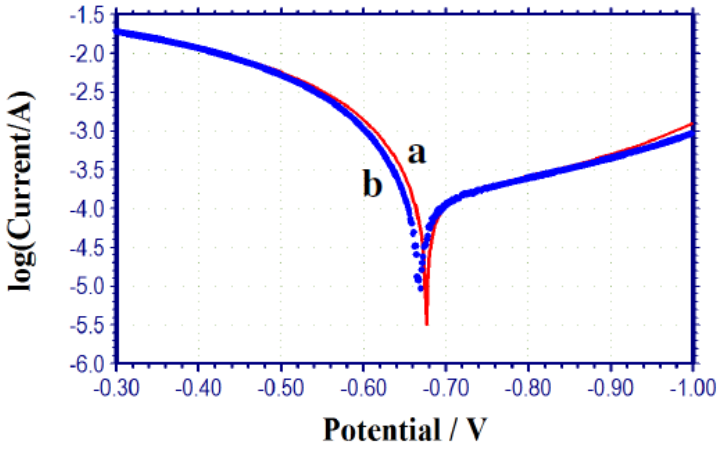

Figure 2. Polarization curves of carbon steel immersed in various test solution. (**a**) Sea water; (**b**) sea water + SG 250 ppm + Zn $^{2+}$ 75 ppm.

When the inhibitors, namely SG (250 ppm) + Zn^{2+} (75 ppm), are added to sea water, the corrosion potential of carbon steel shifts to the noble side (-676 to -668 mV vs. SCE). This indicates that a film is formed on the anodic sites of the metal surface. This film controls the anodic reaction of metal dissolution ($Fe \rightarrow Fe^{2+} + 2e^-$) by forming Fe^{2+}-SG complex on the anodic sites of the metal surface. Formation of Fe^{3+} -SG complex to some extent cannot be ruled out.

Table 5. Corrosion parameters of carbon steel immersed in sea water in presence of SG–Zn^{2+} system obtained from potentiodynamic polarization study.

System	E_{corr} mV vs. SCE	b_c mV/decade	b_a mV/decade	LPR Ohm cm^2	I_{corr} A/cm^2
Sea water	- 676	362	120	152.8	2.559×10^{-4}
Sea water + SG (250 ppm) + Zn^{2+} (75 ppm)	-668	359	114	179.5	2.090×10^{-4}

The formation of a protective film on the metal surface is further supported by the fact that the LPR value increases from 152.8 to 179.5 Ohm cm^2 and the corrosion current decreases from 2.559×10^{-4} to 2.090×10^{-4} A/cm^2.

Thus, polarization study confirms the formation of a protective film on the metal surface.

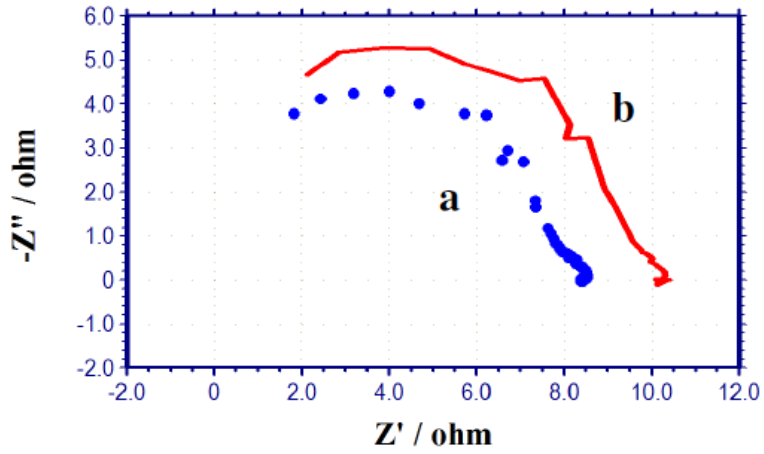

Figure 3. AC impedance spectra of carbon steel immersed in various test solutions (Nyquist plot). (**a**) Sea water; (**b**) sea water + SG 250 ppm + Zn^{2+} 75 ppm.

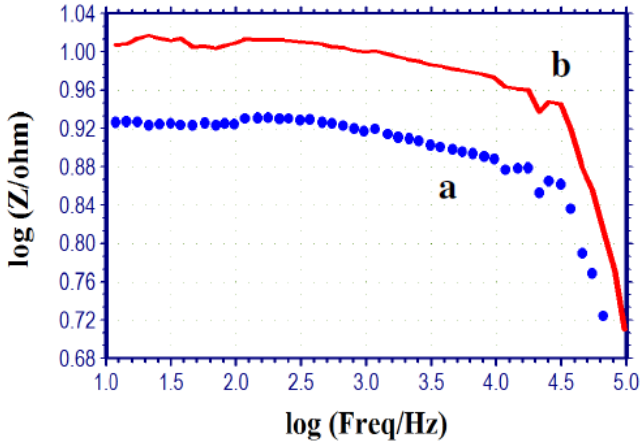

Figure 4. AC impedance spectra of carbon steel immersed in various test solutions (Bode plot). (**a**) Sea water; (**b**) sea water + SG 250 ppm + Zn^{2+} 75 ppm.

AC impedance spectra

AC impedance spectra [Electro chemical impedance spectra] have been used to confirm the formation of a protective film on the metal surface [53-55]. If a protective film is formed on the metal surface, the charge transfer resistance (Rt) value increases; double layer capacitance value (C_{dl}) decreases and the impedance, log (z/Ohm), value increases. The AC impedance spectra of carbon steel immersed in sea water in the presence of the inhibitor system (SG-Zn^{2+}) are shown in Figs. 3 to 5. The Nyquist plots are shown in Fig. 3. The Bode plots are shown in Figs. 4 and 5. The corrosion parameters, namely, R_t, C_{dl} and impedance, log (z/Ohm), values are given in Table 6.

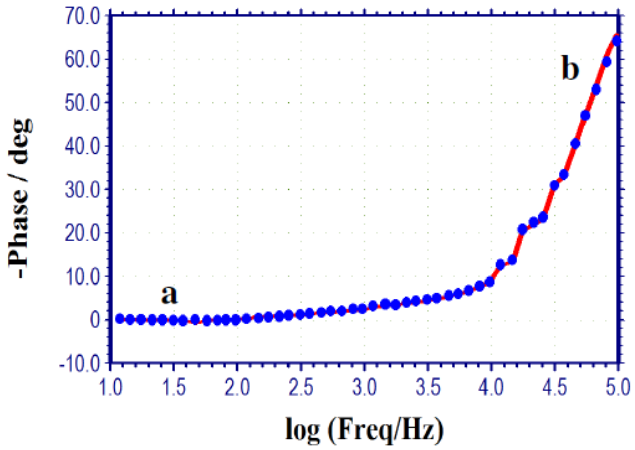

Figure 5. AC impedance spectra of carbon steel immersed in various test solutions (Bode plot). (**a**) Sea water; (**b**) sea water + SG 250 ppm + Zn^{2+} 75 ppm.

When the inhibitors [SG (250 ppm) + Zn^{2+}(75 ppm)] are added to sea water, the R_t value increases from 6.88 to 8.52 Ohm cm^2; the C_{dl} value decreases from 2.849 x 10^{-7} to 2.301 x 10^{-7} F/cm^2; the impedance value increases from 0.9291 to 1.010.

These results lead to the conclusion that a protective film is formed on the metal surface.

Table 6. Corrosion parameters of carbon steel immersed in sea water in presence of SG–Zn^{2+} system obtained from AC impedance spectra.

System	Nyquist plot		Bode plot
	R_t Ohm cm^2	C_{dl} F/cm^2	Impedance, log (Z/Ohm)
Sea water	6.88	2.849 x 10^{-7}	0.9291
Sea water + SG (250 ppm) + Zn^{2+} (75 ppm)	8.52	2.301 X 10^{-7}	1.010

FTIR spectra

FTIR spectra have been used to analyse the protective film formed on the metal surface [50, 56]. The FTIR spectrum (KBr) of pure SG is shown in Fig. 6a. The C=O stretching frequency of the carboxyl group appears at 1631 cm^{-1}.

The FTIR spectrum of the film formed on the metal surface after immersion in sea water containing 250 ppm of SG and 75 ppm of Zn^{2+} is shown in Fig. 6b. The C=O stretching frequency has shifted from 1631 to 1564s cm^{-1}. It is inferred that the oxygen atom of the carboxyl group has coordinated with Fe^{2+}, resulting in the formation of Fe^{2+} - SG complex, formed on the anodic sites of the metal surface. The peak at 3350 cm^{-1} is due to –OH stretching. The band due to Zn-O stretch appears at 1308 cm^{-1}. These results confirm the presence of $Zn(OH)_2$ deposited on the cathodic sites of the metal surface [57].

Thus, FTIR spectral study leads to the conclusion that the protective film consists of Fe^{2+}–SG complex and $Zn(OH)_2$.

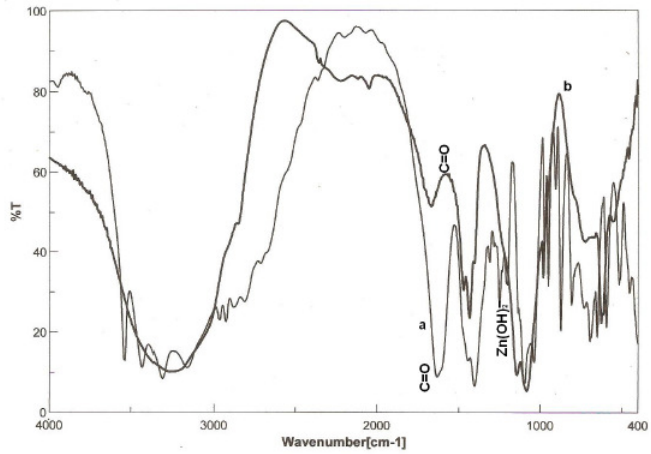

Figure 6. FTIR spectra. **a**. Pure SG; **b**. Film formed on the metal surface after immersion in sea water + SG (250 ppm) + Zn^{2+} (75ppm).

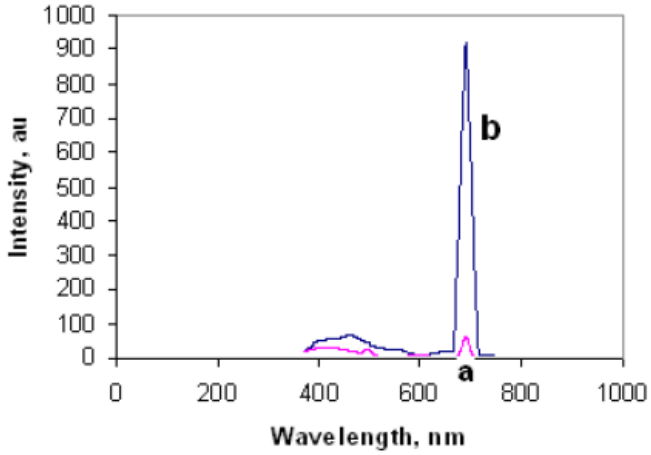

Figure 7. Luminescent spectra for carbon steel immersed in various test solutions using SG as inhibitor. **a**. Fe^{2+} - SG complex; **b**. Protective film formed on the surface of carbon steel after immersion in the solution containing 250 ppm SG and 75 ppm Zn^{2+}.

Luminescence spectra

Luminescence spectra have been used to detect the presence of Fe^{2+} - inhibitor complex formed on the metal surface [51, 57-59].

The luminescence spectrum (λ_{ex} = 230 nm) of the Fe^{2+} -SG complex solution, prepared by mixing aqueous solutions of Fe^{2+} (prepared freshly from $FeSO_4.7H_2O$) and SG, is shown in Fig. 7a. A peak appears at 690 nm.

The luminescence spectrum (λ_{ex} =230nm) of the film formed on the metal surface after immersion in the solution confining 250 ppm of SG and 75 ppm of Zn^{2+} is shown in Fig. 7b. A peak appears at 691 nm. This indicates that the film present on the metal surface consists of Fe^{2+} - SG complex. The slight variation in the position of the peak is due to the fact that the Fe^{2+} - SG complex is entrailed in $Zn(OH)_2$ present on the metal surface. Further, the increase in intensity of the peak is due to the fact that the metal surface after the formation of the protective film is very bright, and the film is very thin and there is enhancement in the intensity of the peak [59].

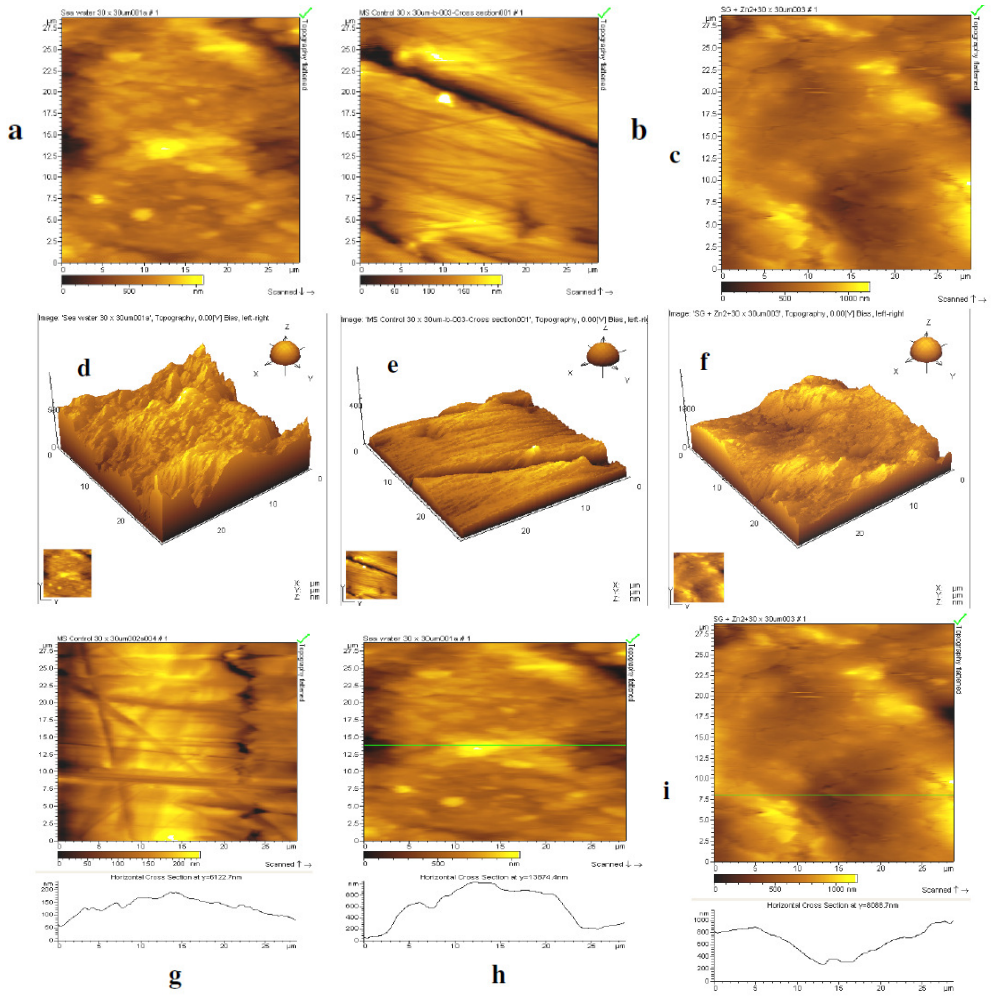

Figure 8. Two dimensional images of surface of: (**a**) polished carbon steel (control); (**b**) carbon steel immersed in sea water (blank); (**c**) carbon steel immersed in sea water containing 250 ppm SG and 75 ppm Zn^{2+}. Three dimensional images of surfaces of: (**d**) polished carbon steel (control); (**e**) carbon steel immersed in sea water (blank); and (**f**) carbon steel immersed in sea water containing 250 ppm SG and 75 ppm Zn^{2+}. The cross-sectional profiles (shown as broken lines) corresponding to the AFM images of surface of: (**g**) polished carbon steel (control), (**h**) carbon steel immersed in sea water (blank), and (**i**) carbon steel immersed in sea water containing 250 ppm SG and 75 ppm Zn^{2+}.

Atomic Force Microscopy

Atomic force microscopy is a powerful technique for the gathering of roughness statistics from a variety of surfaces [60]. AFM is becoming an accepted method of roughness investigation [61]. All atomic force microscopy images were obtained on PicoSPM I Molecular Imaging, USA, AFM instrument operating in contact mode in air. The scan size of all the AFM images is 30 µm x 30 µm area at a scan rate of 2.4 lines per second.

The two-dimensional and three-dimensional AFM morphologies and the AFM cross sectional profile for polished carbon steel surface (reference sample), carbon steel surface immersed in sea water (blank sample) and carbon steel

surface immersed in sea water containing 250 ppm SG and 75 ppm Zn^{2+} are shown in Fig. 8 (a,d,g), (b,e,h), (c,f,i), respectively.

Root mean square roughness, average roughness, and peak to valley value

AFM image analysis was performed to obtain the average roughness, R_a (the average deviation of all points roughness profile from a mean line over the evaluation length), the root-mean-square roughness, R_q (the average of the measured height deviations taken within the evaluation length and measured from the mean line) and the maximum peak to valley (P-V) height values (largest single peak-to-valley height in five adjoining sampling heights) [62]. R_q is much more sensitive than R_a to large and small height deviations from the mean [63].
Table 7 is a summary of the average roughness R_a, rms roughness (R_q), and maximum peak to valley height (P-V) value for carbon steel surface immersed in different environments. The values of R_q, R_a and P-V height for the polished carbon steel surface (reference sample) are 262 nm, 211 nm and 1200 nm, respectively. This shows that the surface is more homogenous, with some places where the height is lower than the average depth. Fig. 8 (a, d, g) displays the non-corroded metal surface. The slight roughness observed on the polished carbon steel surface is due to atmospheric corrosion. The rms roughness, average roughness and P-V height values for the carbon steel surface immersed in sea water are 765 nm, 645 nm and 3700 nm, respectively. These values suggest that carbon steel surface immersed in sea water has a greater surface roughness than the polished metal surface, indicating that the unprotected carbon steel surface is rougher due to the corrosion of carbon steel in sea water environment. Fig. 8. (b, e, h) displays corroded metal surface with few pits.

Table 7. AFM data for carbon steel immersed in inhibited and uninhibited environments.

Samples	RMS(R_q) Roughness (nm)	Average (R_a) Roughness (nm)	Maximum peak to valley height (nm)
Polished carbon steel (blank)	262	211	1200
Carbon steel immersed in sea water (blank)	765	645	3700
Carbon steel immersed in sea water containing 250 ppm SG and 75 ppm Zn^{2+}	470	386	2200s

The formulation consisting of 250 ppm SG and 75 ppm Zn^{2+} in sea water shows R_q value of 470 nm and the average roughness is significantly reduced to 386 nm when compared with 645 nm for carbon steel surface immersed in sea water. The maximum peak to valley height was also reduced to 2200 nm. These parameters confirm that the surface appears smoother. The smoothness of the surface is due to the formation of a protective film of Fe^{2+}- SG complex and Zn $(OH)_2$ on the metal surface thereby inhibiting the corrosion of carbon steel. The above parameters are also somewhat greater than the AFM data of polished metal surface, which confirms the formation of a film on the metal surface, which is protective in nature.

Mechanism of corrosion inhibition

Analysis of the results of weight-loss method reveals that the formulation consisting of sea water, 250 ppm of SG and 75 ppm of Zn^{2+} offers an IE of 98%. Results of polarization study suggest that the formulation functions as cathodic inhibitor. The AC impedance spectral studies indicate that a protective film is formed on the metal surface. FTIR spectra reveal that the protective film consists of Fe^{2+}–SG complex and $Zn(OH)_2$.

In order to explain all these observations in a holistic way, the following mechanism of corrosion inhibition is proposed.

- When carbon steel specimen is immersed in an aqueous solution, the anodic reaction is

$$Fe \rightarrow Fe^{2+} + 2e^-$$

and the cathodic reaction is

$$2H_2O + O_2 + 4e^- \rightarrow 4\ OH^-.$$

- When the system containing 250 ppm of SG and 75 ppm of Zn^{2+} is prepared, there is formation of Zn^{2+}–SG complex

$$Zn^{2+} + SG \rightarrow Zn^{2+}\text{–}SG$$

- When carbon steel is immersed in the solution, the Zn^{2+}–SG diffuses from the bulk of the solution to the metal surface.

- On the surface of metal, Zn^{2+}–SG complex is converted into Fe^{2+} - citrate complex at the local anodic regions. The stability of Fe^{2+}–SG complex is higher than the corresponding zinc complex

$$Zn^{2+}\text{–}SG + Fe^{2+} \rightarrow Fe^{2+}\text{–}SG + Zn^{2+}$$

- The released Zn^{2+} ions combine with OH^- ions to form $Zn(OH)_2$ on the cathodic sites

$$Zn^{2+} + 2\ OH^- \rightarrow Zn(OH)_2\downarrow$$

Thus the protective film consists of Fe^{2+} - SG complex and $Zn(OH)_2$.

Conclusions

The present study leads to the following conclusions:

- A synergistic effect exists between SG and Zn^{2+} in controlling corrosion of carbon steel immersed in sea water.
- The formulation consisting of 250 ppm of SG and 75 ppm offers 98% IE.
- Polarization study suggests that the combination of SG and Zn^{2+} functions as an anodic inhibitor.
- AC impedance spectra reveal that a protective film is formed on the metal surface.
- FTIR spectra show that the protective film consists of Fe^{2+}- SG complex and $Zn(OH)_2$.
- The IE of inhibitor formulation depends on the ability of the inhibitor to form complex with Zn^{2+} and ability of Fe^{2+} to react with Zn^{2+} to form iron complex.
- This formulation may find applications in cooling water systems.
- AFM images and luminescent spectra confirm the formation of a protective layer on the metal surface.

- The synergistic formulation with 250 ppm of CTAB has 91% corrosion inhibition efficiency and 100% biocidal efficiency.

References

1. Gunasekaran G, Dubey BI, Rangarajan J. Def Sci J. 2005;55:51.
2. Ibrahim MAM, Abd El Rehim SS, Abd El Wahaab SM, et al. Plat Surf Finish. 1999;86:69.
3. Oguzie EE, Akalezi CO, Enenebeaku CK, et al. Chem Eng Commun. 2011;198:46.
4. Gharahcheshmeh MH, Sohi MH. J Appl Electrochem. 2010;40:1563.
5. Abboud Y, Abourriche A, Saffaj T, et al. Desalination. 2009;237:175.
6. Oguzie EE. Chem Eng Commun. 2009;196:591.
7. Demadis KD, Papadaki M, Raptis RG, et al. Chem. Mater. 2008;20:4835.
8. Yazdzad AR, Shahrabi T, Hosseini MG. Mater Chem Phys. 2008;109:199.
9. Shahrabi T, Yazdza A, Hosseini M. J Mater Sci Technol. 2008;24:427.
10. Selvi JA, Rajendran A, Amalraj AJ. Indian J Chem Technol. 2007;14:382.
11. Dhanalakshmi J, Arockiaselvi J, Amalaraj AJ, et al. Trans Soc Adv Electrochem Sci Technol. 2006;41:57.
12. Santos LMM, Lacroix JC, Ching KIC, et al. J Electroanal Chem. 2006;587:67.
13. Sowska AT, Kruszynski R. Pol J Chem. 2005;79:1155.
14. Rashwan SM, El-Maksoud SAA, El-Wahaab SMA, et al. Bull Electrochem. 2005;21:199.
15. Chambers BD, Taylor SR, Kendig MW. Corrosion. 2005;61:480.
16. Holmberg VC, Rasch MR, Korgel BA. Langmuir. 2010;26:14241.
17. Madani A, Nessark B, Brayner R, et al. Polymer. 2010;51:2825.
18. Boisier G, Lamure A, Pebere N, et al. Surf Coat Technol. 2009;203:3420.
19. Spah M, Spah DC, Deshwal B, et al. Corros Sci. 2009;51:1293.
20. Gabr IM, El-Asmy HA, Emmana MS, et al. Transition Met Chem. 2009;34:409.
21. Dudukcu M, Udum YA, Ergun Y, et al. J Appl Polym Sci. 2009;111:1496.
22. Okafor PC, Liu CB, X. Liu X, et al. J Appl Electrochem. 2009;39:2535.
23. Quartarone G, Battilana M, Bonaldo L, et al. Corros Sci. 2008;50:3467.
24. Cao YQ, Zhang Z, Guo YX. J Chem Technol Biotechnol. 2007;83:1441.
25. Xia MZ, Wang FY, Lei W, et al. Acta Petrolei Sinica. 2008;24:460.
26. Romanszki L, Telegdi J, Kalman E. Colloids Surf A. 2008;321:20.
27. Jacques S, Rocca E, Stebe MJ, et al. Surf Coat Technol. 2008;202:3878.
28. Xia M, Wang F, Lei W, et al. J Chem Ind Eng. 2008;59:982.
29. Zhou L, Yan J, Gao X. Petroleum Proc Petrochem. 2008;39:63.
30. Matulkova I, Nemec I, Teubner K, et al. J Mol Struct. 2008;873:46.
31. Abulkibash A, Khaled M, El Ali B, et al. Arab J Sci Eng. 2008;33:29.
32. Ochoa N, Pebere N, Tribollet B. ECS Trans. 2006;1:207.
33. Quartarone G, Bonaldo L, Tortato C. Appl Surf Sci. 2006;252:8251.
34. Ein-Eli Y, Auinat M. Meeting Abstracts MA. 2005;2005-02:584.
35. Yurt A, Bereket G, Ogretir C. J Mol Struct: THEOCHEM. 2005;725:215.

36. Wranglen G. Introduction to corrosion and protection of metals. London, UK: Chapman and Hall; 1985. P.236.
37. Shanthy P, Rengan P, Chelvan AT, et al. I J Chem Tech. 2009;16.
38. Rajendran S, Apparao BV,Palaniswamy N. J Electrochem Soc India. 1999;48:89.
39. Rajendran S, Apparao BV, Palaniswamy N. Bull Electrochem. 1997;13:441.
40. Holness RJ, Williams G, Worsley DA et al. J Electrochem Soc. 2005;152:B73.
41. Telegdi J, Shaglouf MM, Shaban A, et al. Electrochim Acta. 2001;46:3791.
42. Selvi JA, Rajendran S, Jeyasundari J. Zastita Materijala. 2009;50:91.
43. Selvaraj SK, Kennedy AJ, Amalraj AJ, et al. Corros Rev. 2004;22:219.
44. Gomma GK. Mater Chem Phys. 1998;55:241.
45. Aramaki K, Hackerman N. J Electrochem Soc. 1969;116:568.
46. Quraishi MA, Rawat J, Ajmal M. Corrosion 1999;55:919.
47. Kanimozhi SA, Rajendran S. Int J Electrochem Soc. 2009;4:353.
48. Roque JM, Pandiyan T, Cruz J, et al. Corros Sci. 2008;50:614.
49. Benali O, Larabi L, Traisnel M, et al. Appl Surf Sci. 2007;253:6130.
50. Amar H, Braisaz T, Villemin D, et al. Mater Chem Phys. 2008;110:1.
51. J. Arockia Selvi, Susai Rajendran, V. Ganga Sri, A. John Amalraj, B. Narayanasamy, Port Electrochim Acta. 2009;27:1.
52. Rajendran S, Paulraj J, Rengan P, et al. J Dent Oral Hyg. 2009;1:001.
53. Zhang S, Tao Z, Li W, et al. Appl Surf Sci. 2009;255:6757.
54. Heakal FT, Fouda AS, Radwan MS. Mater Chem Phys. 2011;125:26.
55. Rajendran S, Devi MK, Regis APP, et al. Zastita materijala. 2009;50:131.
56. Sathiyabama J, Rajendran S, Selvi JA, et al. Open Corros J. 2009;2:76.
57. Kalaivani R, Narayanaswamy B, Selvi JA, et al. Port Electrochim Acta. 2009;27:177.
58. Rajendran S, Apparao BV, Palaniswamy N. J Electrochem Soc, India. 1998;47:43.
59. Rajendran S., Apparao BV, Palaniswamy N. Anti-Corros Met Mater. 1996;46:23
60. Vera R, Schrebler R, Cury P, et al. J Appl Electrochem. 2007;37:519.
61. Dumas Ph, Butfffakhreddine B, Am C, et al. Europhys Lett. 1993;22:717.
62. Thomas TR. Rough surfaces. New York: Longman; 1982.
63. Stout KJ, Sullivan PJ, Mc Keown PA. Annals CRIP. 1992;41:621.